ORIGINAL PAPER

Preparation and clay tolerance research of a polycarboxylate superplasticizer modified by phosphonate group

Ming Zhang[1] · Chunfang Guo[2] · Qian Zhang[1] · Meishan Pei[3]

Abstract

At present, controlling the workability of concrete with high clay content sand presents a significant engineering challenge. A novel phosphonate group-modified polycarboxylate superplasticizer (PHS-PCE) was synthesized by using 2-(methacryloyloxy) ethyl phosphate (MOEP), isobutyl alcohol polyoxyethylene ether (IPEG) and acrylic acid (AA). Gel permeation chromatography (GPC), Fourier-transform infrared spectroscopy (FT-IR), ^{31}P nuclear magnetic resonance (^{31}P NMR) spectroscopy and elemental analysis measurements were conducted to characterize the molecular structure of PHS-PCE showing successful incorporation of the phosphonate group with high polymer purity. Despite the relatively low reactivity of MOEP, approximately 65 wt% monomer was incorporated into the copolymer. PHS-PCE exhibited superior flowability and stronger retardation effect than the conventional polycarboxylate superplasticizer (C-PCE), due to the increased negative charge density and enhanced complexing capacity with calcium ion imparted by the phosphonate group. In the presence of clay, the maximum variation of PHS-PCE adsorption on cement particle was 18%, whereas that of C-PCE was 25%. The phosphonate group facilitates adsorption of a portion of PHS-PCE on the clay particle edges, thereby preventing intercalation and improving the clay tolerance.

Keywords Polycarboxylate superplasticizer · Phosphonate group · Absorption · Clay tolerance

Introduction

Concrete is a major construction material composed of cement, sand, aggregate, water, and admixture, which has become the foundation of modern society. With the increasing scale of construction in our country, high quality natural sand is becoming scarce, leading to a gradual reliance on high clay content sand as the main source of fine aggregate [1]. The main component of clay in sand is montmorillonite (MMT), which can significantly consume polycarboxylate superplasticizer (PCE) through physical and chemical adsorption [2, 3]. Its adsorption amount is approximately 13 times larger than the adsorption on cement [4], resulting

in the reduced flowability, significant slump loss, lower strength and poorer durability in concrete [5, 6].

Based on the molecular structure design, the clay tolerance performance of PCE can be achieved by adjusting the length and morphology of PCE side chains, and introducing functional groups. Lei et al. [7] synthesized a short side chain terpolymer using 4-hydroxybutyl vinyl ether (HEVE) as a functional monomer. Compared with conventional PCE (C-PCE), the short side chains of this polymer limited its intercalations with MMT. However, its dispersibility was poor duo to the reduction of the steric repulsion. Xu et al. [8] prepared a novel PCE with β-cyclodextrin (β-CD) as a side chain, primarily improving the clay tolerance effect through the steric hindrance generated by β-CD. Similarly, Li et al. [9] used modified β-CD as a monomer to synthesize clay-resistant type PCE, which exhibited good fluidity and retardation effect in the presence of clay. Nevertheless, this modified PCE requires the preparation of functional precursors, which complicates the synthesis process and reduces the yield of the product. Currently, sulfonic group as a functional group can significantly increase the absolute value of the zeta potential, enhancing its dispersion and water-reducing abilities in cement-clay systems

✉ Ming Zhang
zm0715@163.com

1 School of Architecture and Engineering, Zibo Vocational Institute, Zibo 255300, China

2 Shan Dong Vocational College of Light Industry, Zibo 255300, China

3 School of Chemistry and Chemical Engineering, University of Jinan, Jinan 250022, China

[10]. Whereas, the introduction of the sulfonic group also leads to a rapid loss in fluidity.

Phosphonate group can enhance its binding capacity with calcium ions, when incorporated into the molecular structure of PCE, promoting greater adsorption of PCE onto cement particle and reducing its susceptibility to clay [11]. Stecher et al. [12] synthesized a phosphonate-modified PCE using 2-(methacryloyloxy) ethyl phosphate (MOEP), methoxy polyethylene glycol methacrylate (MPEGMA) and methacrylic acid (MAA). Compared to the conventional PCE (C-PCE), this modified PCE displayed better dispersibility, stronger retarding effects on cement, and better clay tolerance. However, the limited availability of MPEGMA monomer restricts its application. Wang [13] employed MOEP, isobutyl alcohol polyoxyethylene ether (IPEG) and MAA as raw materials to prepare a phosphonate-modified PCE. However, this study only explored the raw material ratios and process parameters, without further investigation into the superplasticizer's molecular structure and its performance on cement.

Using MOEP as the phosphonate group provider, acrylic acid (AA), and IPEG as reactant monomers, phosphonate-modified polycarboxylate superplasticizer (PHS-PCE) was synthesized via free radical copolymerization. The influence of MOEP dosages on the dispersibility of PHS-PCE was investigated, and the performance of PHS-PCE in cement was also systematically studied. Furthermore, the clay tolerance properties and principles of PHS-PCE were discussed, aiming to provide insights for the preparation of concrete with high clay content sand.

Experimental

Materials

AA ($\geq 99\%$), ammonium persulfate (APS, $\geq 99\%$), ascorbic acid (VC, $\geq 99\%$), 3-mercaptopropionic acid (MPA, $\geq 98\%$), sodium hydroxide (NaOH, $\geq 99\%$): analytical grade, Aladdin Biochemical Technology Co., Ltd; MOEP ($\geq 90\%$): analytical grade, Sigma-Aldrich (USA); sodium montmorillonite (MMT): analytical grade, Tianjin Guangfu Fine Chemical Co., Ltd.; IPEG2300 (M = 2300 g/mol, $\geq 99\%$ purity): Liaoning Oxiranchem Co., Ltd.

Reference cement P.I 42.5: China United Cement Group Co., Ltd., with a chemical composition as shown in Table 1 and compliance with the Chinese Standard GB175-2007, the density is 3.16 g/cm^3.

Synthesis of PCE

The synthesis procedure of C-PCE and PHS-PCE is as follows: Initially, some amount of IPEG and deionized water were added to a four-neck round-bottom flask equipped with mechanical stirrer, reflux condenser, and N$_2$ inlet tube. N$_2$ was bubbled for 30 min to remove dissolved O$_2$, followed by raising to the designed temperature. In the second step, APS was added into the flask to initiate the reaction. Subsequently, AA or (AA and the range amounts of MOEP) was dissolved in deionized water as solution I, and continuously added to the flask at a constant rate within 180 min. Simultaneously, a certain amount of VC and MPA was dissolved in deionized water as solution II, and added to the flask at a constant rate for 210 min. Fourthly, after the completion of solution II addition, stirring was continued for another 60 min at the designed temperature. Finally, PCE was naturally cooled to 25 oC, and then adjusted to a pH of 7.0 using NaOH. The n (MOEP) was 0 mol%, 0.1 mol%, 0.2 mol%, 0.3 mol%, 0.4 mol% and 0.5 mol% based on the IPEG amount of substance respectively, while n(AA): n(IPEG) was 1.0:4.0, and the amounts of APS, VC, and MPA were 1.5 wt%, 0.5 wt%, and 0.5 wt% based on the macro-monomer mass, respectively, at 60° C. The molecular structural formula of C-PCE and PHS-PCE are shown in Fig. 1.

Purification of PCE

The purpose of purification is to remove unreacted unsaturated monomers to accurately characterize the molecular structure of PCE and reflect its true performance. The PCE was purified using a dialysis membrane with a cutoff molecular weight of 5,000 Da. During the purification process, deionized water was replaced every 4–6 h lasted for 72 h to remove the unreacted monomers. The copolymer was dried at 60 °C under vacuum for 24 h until a constant weigh was achieved. The refined PCE is used to conduct all the characterizations and measurements except GPC analysis.

Characterizations of PCE

Gel permeation chromatography (GPC)

The molecular weight (Mw and Mn) and polydispersity index (PDI) of the unpurified PCE were determined using an Agilent 1260 gel permeation chromatography system. To analyze the residual amount of the monomers and the yield of the product using the area normalization method. A refractive index

Table 1 Chemical compositions of reference cement (wt%)

CaO	SiO$_2$	Al$_2$O$_3$	Fe$_2$O$_3$	MgO	f-CaO	Na$_2$O	SO$_3$	loss
65.23	21.02	4.34	3.26	1.83	0.70	0.58	0.47	1.66

Fig. 1 Molecular structural formula of PCE: **a** C-PCE; **b** PHS-PCE

(a) C-PCE   (b) PHS-PCE
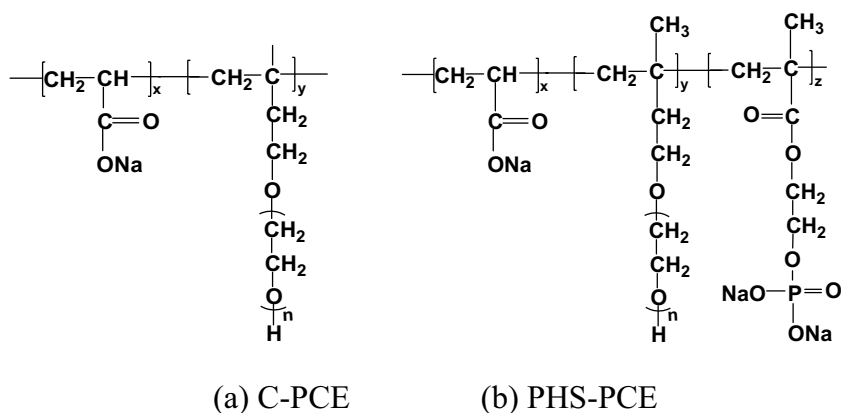
detector was utilized, with 0.1 mol/L $NaNO_3$ as the mobile phase and a series of polyethylene glycol standards with different molecular weight and narrow molecular weight distribution.

Fourier transform infrared (FT-IR)

After KBr and PCE were dried, some amount of KBr was ground with the PCE sample. The mixture was pressed into transparent pellets and placed in the Bruker Vertex 70 FT-IR spectrometer, measuring in the range of $400 \sim 4000$ cm^{-1}.

^{31}P nuclear magnetic resonance (^{31}P NMR)

The ^{31}P NMR spectrum of PHS-PCE sample was recorded on a Bruker ARX-400 spectrometer operating at 25 °C and 162.0 MHz.

Elemental analysis

The phosphorus (P) content in PHS-PCE was determined using an Inductively Coupled Plasma Optical Emission Spectrometer (ICP-OES). A sample of 0.1 g PHS-PCE was placed in a TF container. To this, 8 mL of 65 wt% nitric acid and 2 mL of 30 wt% hydrogen peroxide were added. The mixture was subjected to microwave decomposition at 180 °C for 30 min. The resulting solution was transferred to a 100 mL volumetric flask and diluted to the final volume. For the ICP analysis, an ICAP-6300 ICP-OES (Thermo Fisher, United States) was employed. The instrument operated with the following parameters: RF power at 1150 W, auxiliary gas flow at 0.5 L/min, nebulizer gas flow at 0.5 L/min, and pump speed at 50 rpm. A blank sample, without PHS-PCE, was processed in the same manner for comparison.

Anionic charge density

10.0 g of 20 wt% PCE solution was diluted with 50 mL of deionized water and then acidified using concentrated HCl. During the acidification process, concentrated HCl was added dropwise until the pH reached 1.5. The acidified sample was titrated using a ZDJ-4A automatic potential titrator with 0.5 mol/L KOH solution until the pH reached $12 \sim 13$, which two inflection points corresponding to the chemical equilibrium were observed. The anionic charge density of PCE can be calculated based on the volume difference of KOH solution at the two inflection points [14].

Performance of PCE

Cement dispersibility

The dispersibility of cement was evaluated according to the national standard GB/T 8077–2012 using a truncated cone mold. The water to cement ratio (w/c) was 0.29, and the dosage of PCE from 0.04 to 0.22 bwoc% (based on the weight of cement). After 1 h, the fluidity of the cement paste with 0.18 bwoc% PCE was measured. To assess the effect of MMT on the dispersibility of cement paste, 1.0 bwoc% or 2.0 bwoc% MMT was thoroughly mixed with cement, and then tested following the aforementioned procedure.

Adsorption on cement

The adsorption of PCE on cement was tested using the Shimadzu TOC-5000A total organic carbon analyzer [15]. The quantity of PCE' adsorption was calculated based on the difference of the concentration observed in the suspension.

a. Thermodynamic adsorption of PCE on cement: In a 50 mL conical flask, some amount of PCE, 10.0 g of cement, and 5.0 g of deionized water were thoroughly mixed. The flask oscillated on a constant temperature shaker at 25°C for 120 min. Subsequently, the mixture was separated in a TG16-WS high speed centrifuge at 8000 rpm for 10 min. After centrifugation, some amount of supernatant was filtered using a 0.45 μm filter membrane and diluted with deionized water. The TOC content of solution was then measured.

b. Kinetic adsorption of PCE on cement: In a 50 mL conical flask, a quantified amount of PCE (0.2 bwoc%), 10.0 g of cement, and 5.0 g of deionized water were thoroughly mixed. The flask was then placed on a constant temperature oscillator at 25°C and shaken for 10, 30, 60, 90, and 120 min, respectively. After reaching specified time, the TOC measurement was operated following the same procedure as in (a) to evaluate the variation of PCE adsorption on cement particle over time.

c. Adsorption of PCE on MMT: 20.0 g of PCE solution with concentrations from 0 to 2.4 g/L and 1.0 g of MMT were added to a 50 mL conical flask and thoroughly mixed. The flask was placed on a constant temperature oscillator and shaken for 5 min at 25 °C. Subsequently, the mixture was separated at 4000 rpm for 3 min using a TG16-WS high speed centrifuge. The TOC of solution was then measured following the same procedure as in (a).

Zeta potential

0.1 g of cement, various amounts of PCE (0, 0.2 bwoc%, 0.4 bwoc%, 0.6 bwoc%, 0.8 bwoc%, 1.0 bwoc%, and 1.2 bwoc%), and some amount of deionized water (w/c = 200) were thoroughly mixed for 5 min. The zeta potential of the cement suspension was then measured using JS94H micro-electrophoresis instrument at 25 °C.

Hydration heat

To measure the hydration heat of cement paste with or without PCE, the TAM AIR08 calorimeter was used [16]. A mixture of 10.0 g of cement, some amount of PCE (0.2 bwoc%), and a quantity of deionized water (w/c = 0.35) was thoroughly mixed. The mixture was then poured into a glass ampoule, and the hydration heat of the cement paste was recorded over the next 72 h.

Scanning electron microscopy (SEM) characterization of hydrated cement

20.0 g of a C-PCE or PHS-PCE solution with a concentration of 2.4 g/L and 2.0 g of clay were added into a 50 mL centrifugation tube and mixed thoroughly. The tube was placed in a thermostatic shaker and agitated for 10 min at 25 °C. Then, the mixture was separated at 8000 rpm for 10 min using a TG16-WS high-speed centrifuge. Subsequently, the precipitate was collected and dried at 25 °C. For comparison, 20.0 g of deionized water and 2.0 g of clay were mixed and filled into a 50 mL tube, following the same procedure. Finally, the microscopic morphologies of the clay with and without PCE were observed via a Gemini 300 field emission scanning electron microscope (Carl Zeiss Co., Germany) by coating with gold.

Conductivity test

The calcium ion chelating ability of PCE was evaluated through conductivity measurement. 0.2 g of PCE was added to 100 mL solution of $CaCl_2$ with a concentration of 12.5 mg/L stirred for 60 min at 20 ± 2 °C. Subsequently, the conductivity of the $CaCl_2$ solution with and without PCE was measured using a DDS-307 conductivity meter.

Results and discussion

Synthesis parameters of PHS-PCE

Effect of MOEP amount on dispersibility of PHS-PCE

The impact of varying MOEP amount on the dispersibility of cement paste with PHS-PCE was investigated, when n(AA): n(IPEG) was 1.0:4.0, and the amounts of APS, VC, and MPA were 1.5 wt%, 0.5 wt%, and 0.5 wt% based on the macro-monomer mass, respectively, at 60 º C.

Figure 2 indicates that the fluidity of cement paste initially reaches to a plateau and then decreases with an increase in MOEP amount. The application of MOEP makes the absolute value of PHS-PCE's zeta potential bigger due to the phosphonate group carrying two negative charges, leading to enhanced fluidity of cement paste. However, as shown in Fig. 3, the yield of PHS-PCE decreases from 95.7% to 85.84% with increasing MOEP amount. This decrease is attributed to the lower reactivity of MOEP, which reduces the yield of PHS-PCE. The maximum fluidity of cement paste occurs at n(MOEP): n(IPEG) of 0.375:1.0, indicating that the dispersibility of PHS-PCE is influenced by both its yield and molecular structure. When n(MOEP): n(IPEG) exceeds 0.375:1.0, the low yield of PHS-PCE becomes the primary factor affecting copolymer dispersibility, resulting in a decrease in the fluidity of cement paste.
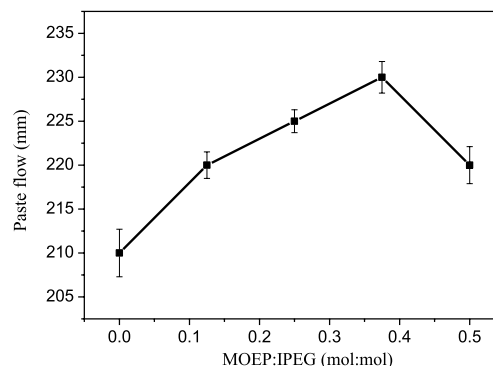

Fig. 2 Effect of the MOEP amount on the dispersibility of cement paste with PHS-PCE
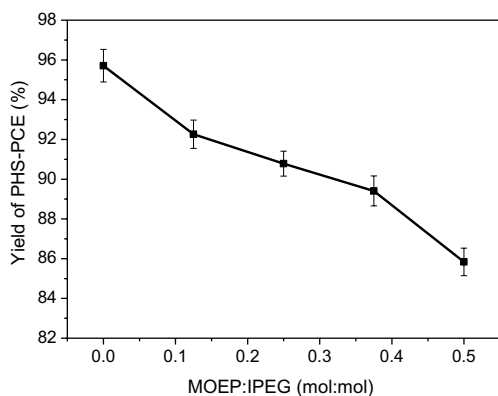
Fig. 3 Effect of the MOEP amount on Yield of PHS-PCE

Effect of APS amount on dispersibility of PHS-PCE

The impact of APS dosage on the dispersion properties of cement paste containing PHS-PCE was investigated. The ratios of the monomers were as follows: n(IPEG): n(AA): n(MOEP) = 1.0: 4.0: 0.375. The amounts of MPA and VC were 0.5 wt% and 0.5 wt% based on the macro-monomer mass at 60 $^{\circ}$ C., respectively.

Figure 4 shows that, as APS dosage increases, the flowability of the cement paste with PHS-PCE initially rises to a maximum value and then decreases. Increasing the dosage of APS results in a higher generation of free radicals, promoting the yield of PHS-PCE and enhancing its dispersing performance. The optimal dispersion of the cement paste with PHS-PCE is observed when the APS dosage is 1.25 wt% based on the mass of the macromonomer. Beyond this APS dosage, the excessive free radicals create additional active sites within the copolymer molecular structure, leading to a reduction in the molecular weight, thereby diminishing its dispersibility.
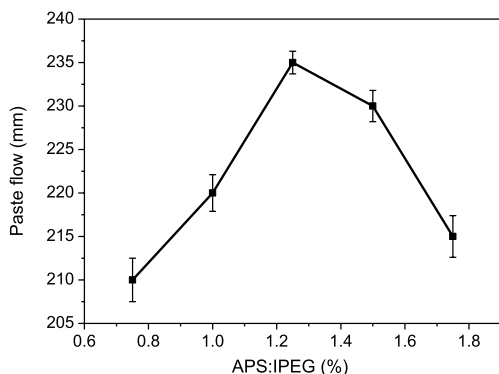
Effect of VC amount on dispersibility of PHS-PCE

The impact of VC dosage on the dispersibility of cement paste with PHS-PCE was investigated. The ratios of the monomers were as follows: n(IPEG): n(AA): n(MOEP) = 1.0: 4.0: 0.375. The amounts of APS and MPA were 1.25 wt% and 0.5 wt% based on the macromonomer mass at 60 $^{\circ}$ C, respectively.

As shown in Fig. 5, the effect of VC dosage on the flowability of cement paste with PHS-PCE follows a tendency similar to that of APS. This is due to the formation of a redox initiation system between VC and APS. At a VC dosage of 0.5 wt% based on the mass of macromonomer mass, the APS-VC system generates an optimal number of free radicals, leading to a moderate molecular weight of PHS-PCE and resulting in excellent dispersing performance. However, further increasing the VC dosage adversely affects the initiation efficiency of the APS-VC system, decreasing the dispersibility of PHS-PCE.

Effect of MPA amount on dispersibility of PHS-PCE

The impact of MPA dosage on the dispersion properties of cement paste containing PHS-PCE was investigated The ratios of the monomers were as follows: n(IPEG): n(AA): n(MOEP) = 1.0: 4.0: 0.375. The amounts of APS and VC were 1.25 wt% and 0.5 wt% based on the macromonomer mass at 60 $^{\circ}$ C, respectively.

Figure 6 illustrates that, as the dosage of mercaptopropionic acid (MPA) increases, the flowability of cement paste with PHS-PCE first increases and then decreases. The MPA dosage primarily affects the main chain length of the copolymer. At an MPA dosage of 0.4 wt% based on the macromonomer mass, PHS-PCE exhibits optimal dispersing performance, indicating that this dosage results in the optimal main chain length of copolymer. Further increasing the MPA dosage shortens the main chain length of PHS-PCE, which adversely affects its dispersing performance.
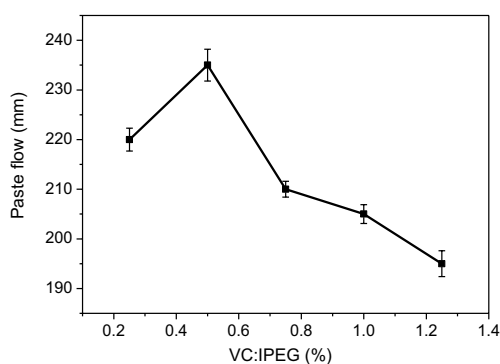

Fig. 4 Effect of the APS amount on dispersibility of cement paste with PHS-PCE

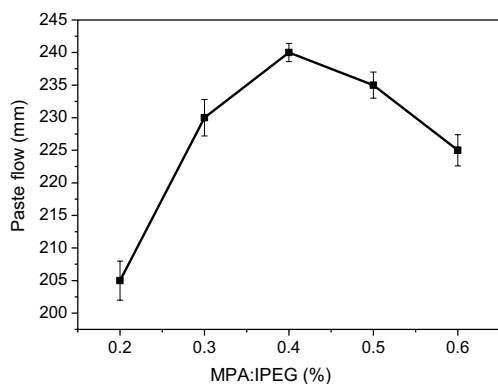**Fig. 5** Effect of the VC amount on dispersibility of cement paste with PHS-PCE

Fig. 6 Effect of the MPA amount on dispersibility of cement paste with PHS-PCE

In summary, the optimal conditions for synthesizing PHS-PCE are determined to be a molar ratio of n(IPEG): n(AA): n(MOEP) = 1.0:4.0:0.375, with amounts of APS, VC, and MPA at 1.25 wt%, 0.5 wt%, and 0.4 wt% of the total macromonomer mass, respectively. The synthesis is conducted at a temperature of 60 °C. Under these conditions, PHS-PCE is synthesized and subjected to structural characterization and performance testing. For comparative purposes, a C-PCE is synthesized with a molar ratio of n(IPEG): n(AA) = 1.0:4.0 and the same synthesis conditions as PHS-PCE.

Characterization of PHS-PCE

Molecular weight analysis

GPC spectra of Unrefined C-PCE and PHS-PCE were performed, showing as Fig. 7, while Table 2 presents the data for the molecular weight and molecular weight distributions (PDI) of the polymers.

In Fig. 7(a) and (b), each exhibits a main peak representing the PCE polymer and a secondary peak representing residual monomers and by-products, indicating high purity of two copolymers. However, the use of MOEP reduces the main chain length of copolymer and broadens its molecular weight distribution. This can be concluded from the weight average molecular weight and PDI values of C-PCE and PHS-PCE in Table 2.

FT-IR analysis

The FT-IR spectrum of PHS-PCE is shown in Fig. 8.

From Fig. 8, the peak at 2882 cm^{-1} represents the stretching vibration of C-H, while the symmetric and stretching vibration peak of -C–O–C appear at 1107 cm^{-1}. The peak at 1725 cm^{-1} is attributed to the characteristic absorption peak of C=O [17]. Peaks at 942 cm^{-1} and 1283 cm^{-1} represent the stretching vibration of P-O [16]. Therefore, the presence of ether group (-C–O–C-), carboxyl group (-COO-), and phosphonate functional group confirms the successful synthesis of PHS-PCE.

^{31}P-NMR analysis

^{31}P-NMR was used to determine the phosphonate functional group in PHS-PCE, as shown in Fig. 9. Figure 9 illustrates that the characteristic peak observed at 0.62 ppm in the ^{31}P NMR spectrum is attributed to the P atom in the O-P–C

Table 2 GPC data regarding the C-PCE and PHS-PCE

Sample	Mw (g/mol)	Mn (g/mol)	PDI (Mw/Mn)
C-PCE	31090	21407	1.45
PHS-PCE	27832	14815	1.88
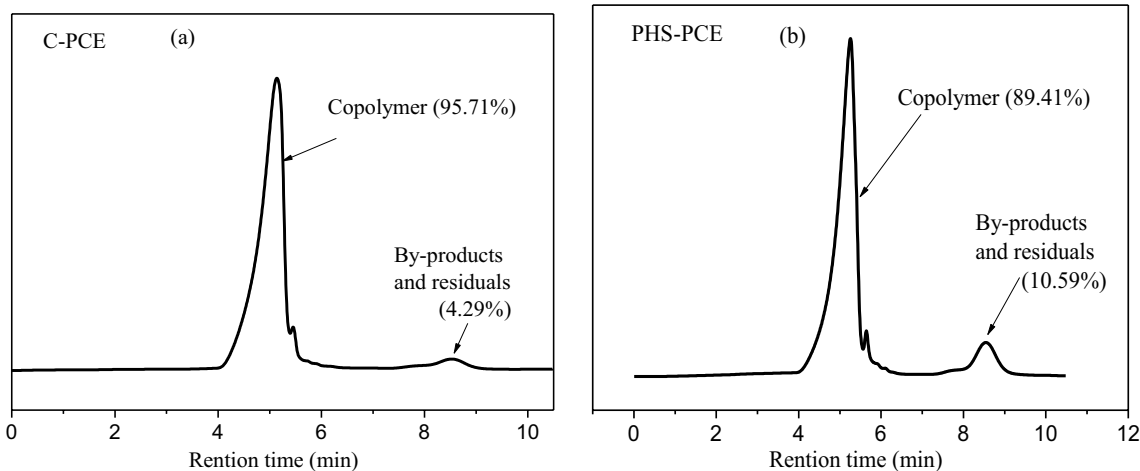
Fig. 7 GPC spectra of samples (**a**) C-PCE; **b** PHS-PCE
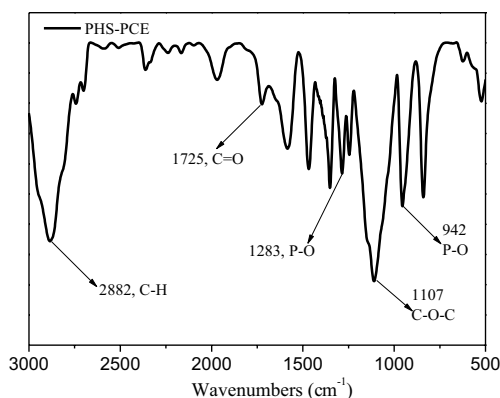
Fig. 8 FT-IR spectra of PHS-PCE

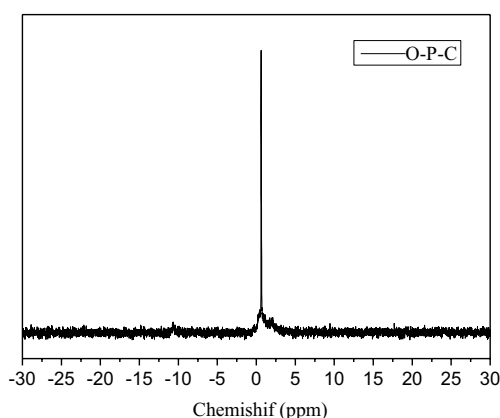**Fig. 9** ^{31}P-NMR spectra of PHS-PCE

bond [18]. Furthermore, it can be inferred that the O-P–C bond is present in the PHS-PCE structure. This confirms the successful introduction of the phosphonate functional group into the copolymer, consistent with the designed PHS-PCE molecular structure.

Elemental analysis

The quantitative content of phosphorus in the copolymer is determined by elemental analysis, and the experimental results are presented in Table 3.

The theoretical phosphorus content calculated from the feed ratio of monomers is 0.44 wt%, whereas the detected phosphorus content in PHS-PCE is 0.29 wt%, which is lower than the theoretical value. This discrepancy can be attributed to the lower reactivity of MOEP monomer compared to other monomers, with only approximately 65 wt% of MOEP monomer being incorporated into the copolymer molecular structure. The lower reactivity of MOEP monomer also contributes to a reduction in the yield of PHS-PCE to some extent.

Table 3 Data of P elemental content in PHS-PCE

Sample	P content (wt%)	
PHS-PCE	Theoretical	0.44
	Analytical	0.29

Table 4 Anion charge density of C-PCE and PHS-PCE

Parameter		C-PCE	PHS-PCE
Anion charge density	mg KOH/g PCE	67	73
	m mol COOH/g PCE	1.20	1.30

Anionic charge density

The anionic charge densities of C-PCE and PHS-PCE are presented in Table 4.

From Table 4, it can be observed that the anion charge density of PHS-PCE is higher than that of C-PCE. This is primarily due to the introduction of phosphonate group into the molecular structure of PHS-PCE, increasing its anion charge density. The anion charge density of PCE plays a significant role in determining its zeta potential and adsorption properties.

Performance of PCE in cement

PCE dosages on the fluidity of cement paste

To evaluate the dispersibility of PCE in cement, the impact of dosage on the flowability of cement paste is investigated, as depicted in Fig. 10.

From Fig. 10, it can be observed that when the dosage of PCE is below 0.18 bwoc%, the initial flowability of cement paste rapidly increases with the addition of both C-PCE and PHS-PCE. However, when the PCE dosage exceeds 0.18 bwoc%, the flowability of cement paste shows a slight increment after reaching the plateau. This is because the added PCE leads to only minor changes in the adsorption on the cement particle after saturation. The maximum flowability of cement paste with PHS-PCE can reach 295 mm, while that of C-PCE is 285 mm. This is attributed to the higher anion density of PHS-PCE compared to C-PCE, resulting from the introduction of phosphonate group into its molecular structure. Abile found that the charge density determines adsorption. When the charge density increases, the adsorption also increases [19]. While, the dispersion effect of the cement paste can be improved by the increasing adsorption of PCE onto the cement particle [20]. The PCE absorbed on the cement particles could form a certain thickness of adsorption layer
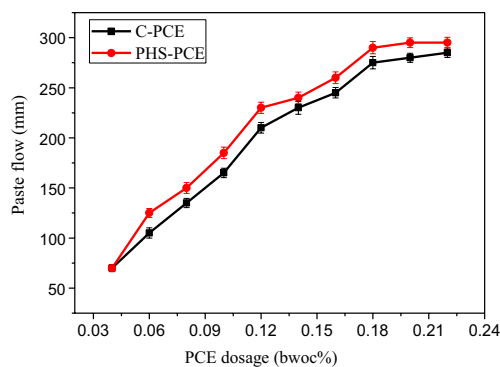
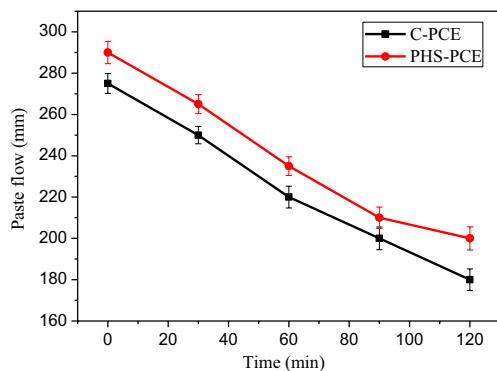**Fig. 10** Effect of PCE dosages on the dispersibility of cement paste

Fig. 11 Spread flow of cement paste with PCE as function of time

and effectively disperse the cement particles through electrostatic repulsion and steric hindrance [21].

Figure 11 shows the flowability retention of cement paste with PCE (0.18 bwoc%) over time. This is because as cement hydration progresses, some of PCE adsorbed on cement particle becomes covered by the hydration layer, resulting in a loss of flowability [22]. PHS-PCE exhibits better flowability

retention of cement paste compared to that of C-PCE owe to its strong chelating ability with calcium ion prolongs the induction period of cement hydration, thereby reducing the rate of cement hydration and beneficial for maintaining the flowability of cement paste [23].

Adsorption behavior on cement

In order to quantitatively analyze the interaction between PCE and cement particle, the adsorption characteristics of PCE on cement particle is conducted, as depicted in Fig. 12.

As shown in Fig. 12(a), when the PCE dosage is below 0.2 bwoc%, the adsorption of PCE rapidly increases with added dosage and then stabilizes. From Fig. 12(b), it can be seen that the maximum adsorption rate of PCE is attained within the first 20 min and then gradually decreases. This is attributed to the combined effects of the consumption of PCE by cement hydration and the continuous adsorption of PCE on cement particle in the solution [24]. Compared to C-PCE, PHS-PCE displays higher anion charge density, which promotes its adsorption on cement particle, resulting in higher saturation adsorption capacity and faster adsorption rate. Plank et al. [25] found a correlation between the dispersibility of superplasticizer and its adsorption capacity, which higher adsorption amount leads to better dispersibility of cement paste.

Zeta potential

The adsorption of PCE on cement particle can be evaluated using the zeta potential. The influence of PCE dosages on the zeta potential of cement particle is illustrated in Fig. 13.

Figure 13 displays that in the absence of PCE, cement particle exhibits a positive zeta potential. Generally, the zeta potential of cement particle depends on the dissolved cement clinker. The hydration products of the aluminate
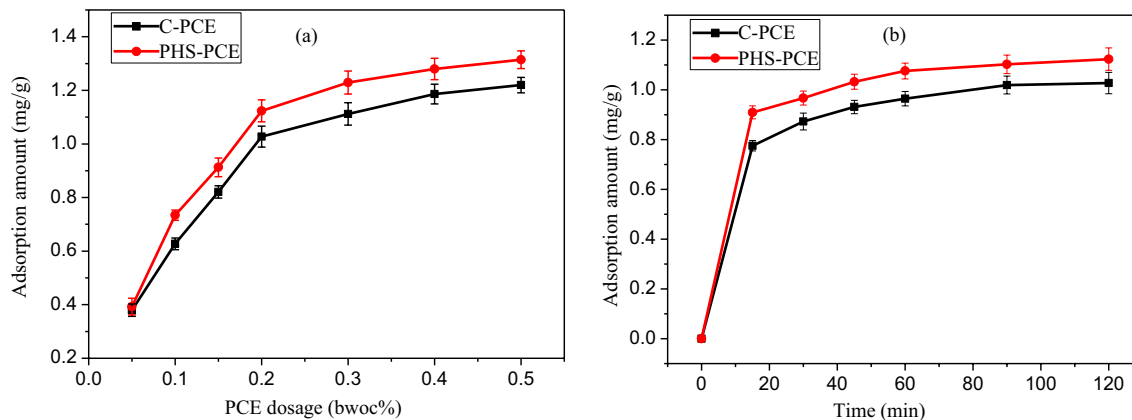

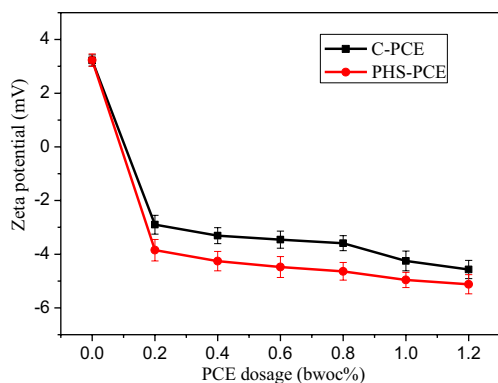**Fig. 12** Adsorption amount of PCE on cement as a function of (**a**) PCE dosage; (**b**) time

Fig. 13 Zeta potential of cement paste as a function of PCE dosages

Fig. 14 Hydration heat of cement paste with and without PCE

phase in the clinker are positively charged, while that of the silicate phase are negatively charged [26]. In the blank cement paste system, the positively charged regions cover most of the cement surface, resulting in an overall positive zeta potential. Upon addition of PCE, superplasticizer molecules can adsorb onto the positively charged regions of cement particle through electrostatic attraction or onto the negatively charged regions via bridging with calcium ions [23], resulting in a shift of the zeta potential from positive to negative. After reaching the saturation adsorption point, no additional PCE molecules continue to adsorb onto the cement particle, thus stabilizing the zeta potential. At the same concentration, PHS-PCE presents a stronger electronegativity compared to C-PCE, attributed to the higher anion charge density introduced by phosphonate group. Moreover, a larger negative zeta potential implies stronger electrostatic repulsion, promoting higher adsorption of superplasticizer and better flowability of cement paste [27].

Hydration heat

The effect of PCE on the hydration heat of cement paste is depicted in Fig. 14.

The Fig. 14 shows that compared to the blank sample, the appearance time of the second peak of hydration heat in cement paste with PCE is delayed. The second peak of hydration heat in the blank cement paste appears around 10.2 h, while for cement pastes with C-PCE and PHS-PCE, the appearance times of the second peak are approximately 15.6 h and 16.0 h, respectively. This indicates that the addition of PCE can delay the hydration process of cement paste [23]. On one hand, the PCE adsorbed on the cement particle impedes the contact between water and cement particle, affecting cement hydration. On the other hand, the complexes formed between carboxyl group and phosphonate group with calcium ions restrict the nucleation and
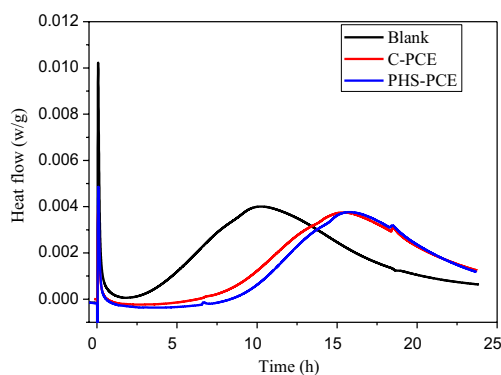
growth of hydration products such as calcium hydroxide (CH), delaying the hydration process of tricalcium silicate [25].

Compared to C-PCE, PHS-PCE exhibits stronger retarding properties. This is attributed to a higher amount of PHS-PCE adsorbed on the cement particle, resulting in a thicker adsorption layer that further impedes the contact between cement particle and water. Additionally, the phosphonate group in PHS-PCE enhance its chelating ability with calcium ions, leading to a greater hindrance to the growth of CH crystals, significantly prolonging the induction period and hydration process of cement paste. The strong retarding effect of PHS-PCE is be beneficial to the retention of the flowability of cement paste.

Calcium ion complexation ability

The chelating ability of PCE with calcium ion can be evaluated through conductivity measurements. The conductivity test results of $CaCl_2$ solution with PCE are illustrated in Fig. 15.

From Fig. 15, it is evident that the addition of PCE reduces the conductivity of the $CaCl_2$ solution. This is attributed to the chelation between carboxyl and phosphonate groups in PCE and calcium ion [28], thereby decreasing the concentration of free calcium ion in the solution and consequently lowering its conductivity. Relative to the conductivity of the blank $CaCl_2$ solution, the addition of C-PCE results in a reduction of 8.2%, while the addition of PHS-PCE leads to a decrease of 11.7% in conductivity. This indicates that the chelating ability of PHS-PCE is stronger than that of C-PCE. The number and types of functional groups in PCE significantly influence the chelating ability with calcium ion [29]. The introduction of phosphonate group in PHS-PCE enhances its chelating capability with calcium ion.
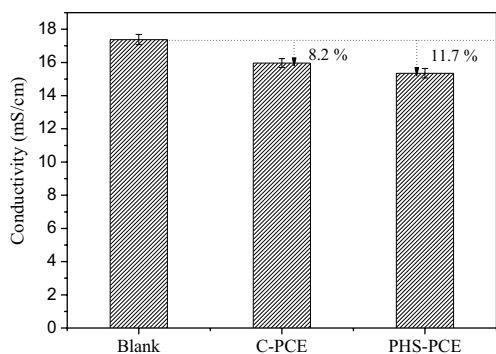
Fig. 15 Conductivity of the CaCl$_2$ solution with and without PCE

XRD analysis

XRD can be used to investigate the growth of main hydration products of cement paste with and without PCE, as shown in Fig. 16.

Figure 16(a) indicates that after 1 day of hydration, the cement paste with PCE exhibits a weaker intensity peak of CH at $2\theta = 18°$ compared to the blank sample, suggesting PCE can inhibit the early hydration of cement. This is attributed to the adsorption of PCE on the cement particle and the chelation of carboxylate and phosphonate groups with calcium ion, which delays the hydration process of cement [30, 31]. This finding is consistent with the experimental results of cement paste hydration heat. Additionally, compared to C-PCE, the phosphonate group in PHS-PCE can lead to higher adsorption and stronger calcium ion chelating capacity, thereby reducing the amount of CH generated obviously. Furthermore, as shown in Fig. 16(b), after 3 days of hydration, the peak intensities of CH in both the blank and PCE-added cement pastes are similar, indicating that PCE has minimal influence on the later strength of cement.

Clay tolerance

To assess the clay tolerance performance of PCE, 1.0 bwoc% or 2.0 bwoc% of MMT was uniformly mixed with cement, and the flowability of the mixture is tested.

As shown in Fig. 17, the flowability of cement paste decreases to varying degrees with MMT dosage increasing. When MMT dosage in cement is 0 bwoc%, 1.0 bwoc%, and 2.0 bwoc%, the flowability of cement pastes with PHS-PCE is respectively 3.6%, 7.5%, and 16% higher than the cement pastes with C-PCE, indicating that the impact of MMT on PHS-PCE is less than that of C-PCE.

Figure 18 indicates that MMT leads to an increase in PCE adsorption, as the PCE's polyethylene glycol side chain enters into interlayer of MMT and forms intercalation, thereby negatively affecting PCE performance [2]. Moreover, from Fig. 15, it also can be observed that the maximum adsorption amount of C-PCE and PHS-PCE increase by 25% and 18% respectively, suggesting that under clay condition, PHS-PCE is more stable and effective compared to C-PCE.
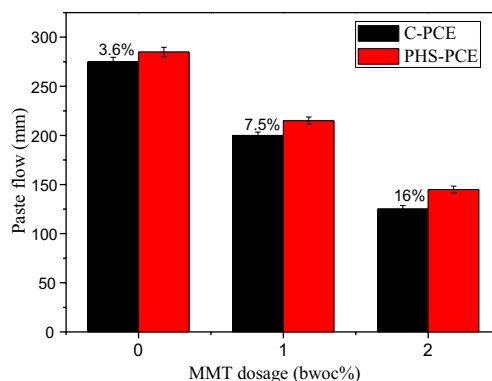

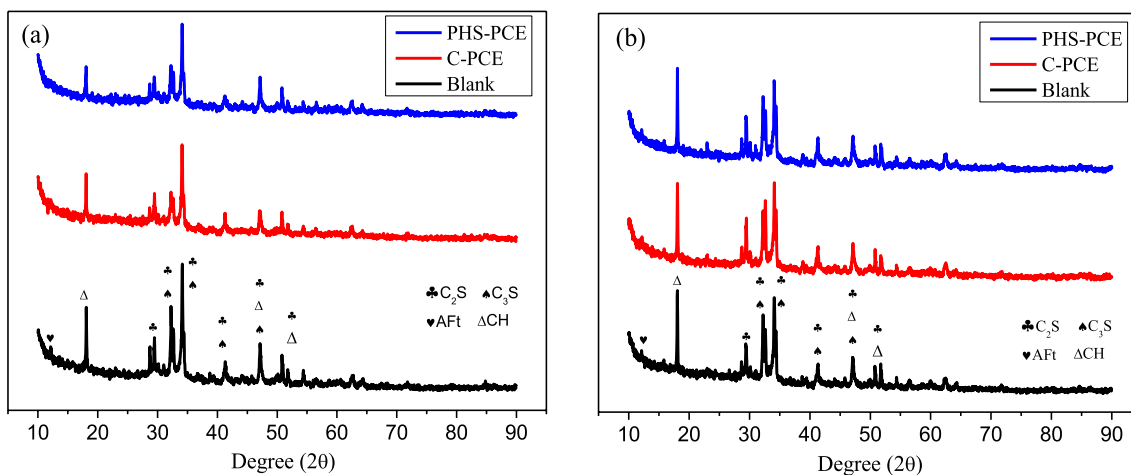**Fig. 17** Effect of MMT on fluidity of cement paste with PCE

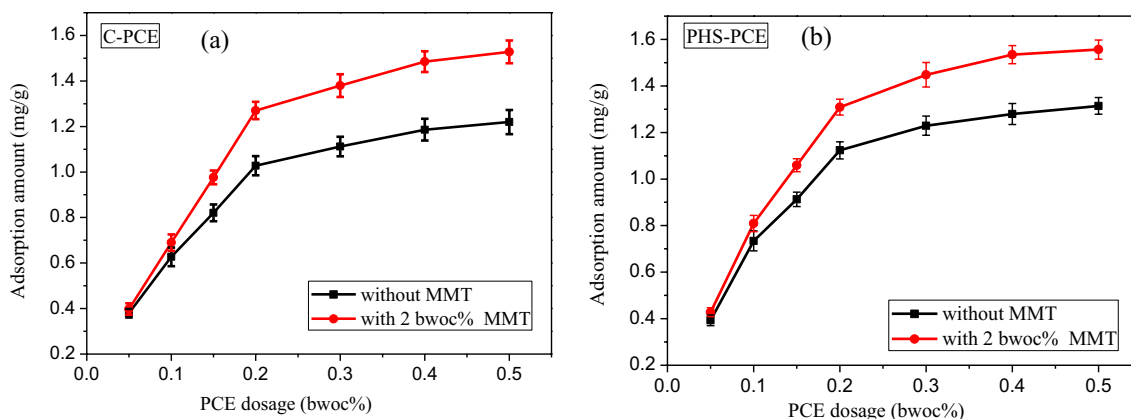**Fig. 16** XRD spectra of hardened cement paste with and without PCE: **a** 1 d; **b** 3 d

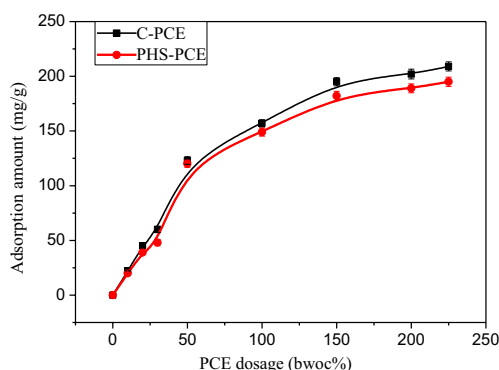**Fig. 18** Adsorption amount of PCE tested with and without MMT: **a** C-PCE; **b** P-PCE

Fig. 19 Adsorption of PCE on MMT

particle for dispersion. Compared to C-PCE, the presence of phosphonate functional group in PHS-PCE results in a higher anionic charge density, leading to the adsorption of some superplasticizer molecules on the edges of MMT. To some extent, this decreases the intercalation of PHS-PCE by MMT, thereby reducing its adsorption amount on MMT.

Dried clay in the absence and presence of PCE are obtained by SEM testing. As shown in Fig. 20(a), block-shaped substances can be observed, which are clay particle aggregates. From Fig. 20(b) and (c), it can be seen that, in addition to the larger clay particle aggregates, there are also smaller clay particles. This is a result of clay particles being dispersed after adsorbing PCE. Compared to C-PCE, more fine particles are observed in clay mixed with PHS-PCE. This is due to the introduction of phosphonate group, which enhance the interaction between PHS-PCE and clay, leading to better dispersion and clay tolerance.

Mechanism of the clay tolerance of PHS-PCE

On the basis of the aforementioned research, the mechanism of the clay tolerance of PHS-PCE is proposed, as shown in Fig. 21.
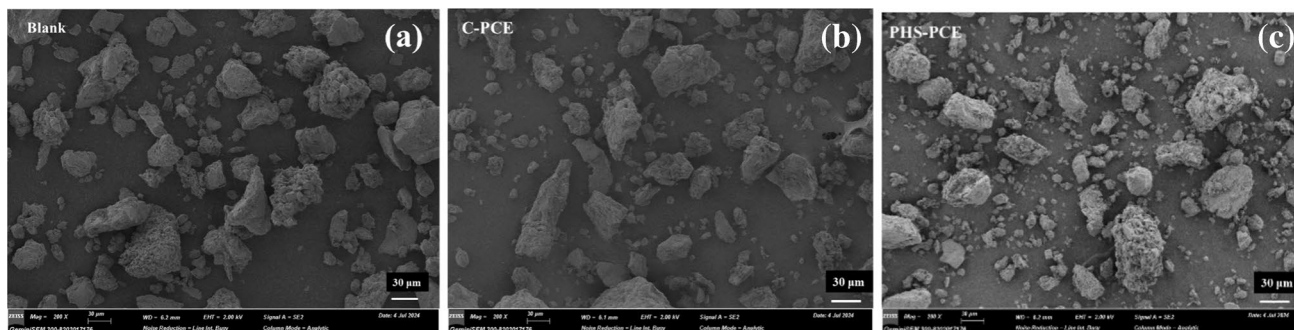
Due to the presence of phosphonate functional group in PHS-PCE, it possesses higher anionic charge density and stronger chelating ability with calcium ion [12], enhancing the correlation between superplasticizer and cement and demonstrating better clay tolerance than C-PCE.

Figure 19 shows that the adsorption of PHS-PCE on MMT is lower than that of C-PCE, meaning that in cement-MMT system, more PHS-PCE molecules are adsorbed by cement

Fig. 20 SEM images of clay with and without PCE (**a**) Blank; **b** C-PCE; **c** PHS-PCE

In the suspension of cement paste, calcium ion is adsorbed onto the negatively charged surface of MMT, rendering it positively charged [6]. PCE molecules, carrying negative charges, are adsorbed onto MMT via electrostatic attraction, as depicted in Fig. 21 (A-a) and (B-a). Hydrogen atom from water molecule adsorbed on the MMT layers can form hydrogen bond with oxygen atom in the PEO side chain of PCE, allowing the side chain to be inserted into the interlayer of MMT and leading to intercalation, which is the primary mode of interaction between PCE and MMT [6], as shown in Fig. 21 (A-b) and (B-b). Stecher et al. [12] considered that incorporating phosphonate group into the structure of superplasticizer increases the affinity between the copolymer and particle. The phosphonate group in PHS-PCE enhances its interaction with MMT particle, causing some PHS-PCE molecules to be adsorbed on the edges of MMT, as illustrated in Fig. 21 (B-c). Due to electrostatic repulsion and steric hindrance, the PHS-PCE adsorbed on the edges of MMT prevents superplasticizer molecules from being intercalated. In contrast, the interaction between carboxyl group and calcium ion is relatively weak, so that C-PCE cannot stably adsorb onto the edges of MMT, resulting in a lack of the mechanism depicted in Fig. 21 (B-c). In summary, compared to C-PCE, PHS-PCE has less intercalation amount, thus exhibiting better clay tolerance performance.

Conclusions

Using IPEG as the macro-monomer, AA as the unsaturated acid monomer, and MOEP as the phosphonate group provider, PHS-PCE was successfully synthesized. The relationship between its structure and property, as clay tolerance performance, was systematically investigated, coming to the following conclusions.

(1) GPC, FT-IR, and ^{31}P NMR measurements confirmed the successful incorporation of the phosphonate group into the molecular structure of copolymer, and PHS-PCE exhibited high purity. Furthermore, the use of MOEP broadened the molecular weight distribution of the superplasticizer, but as the amount of MOEP increased, the yield of the PHS-PCE decreased.

(2) P element content determination demonstrated that although only 65% of the MOEP entered into the copolymer, its possession of two negative charges increased the anionic charge density and calcium ion chelating ability, leading to better fluidity and stronger retarding effects in cement paste with PHS-PCE.

(3) PHS-PCE presents better clay tolerance performance compared to C-PCE. This is attributed to the introduction of phosphonate group in PHS-PCE, which enhances its interaction with particle. On one hand, the adsorption of PHS-PCE on cement particle is less
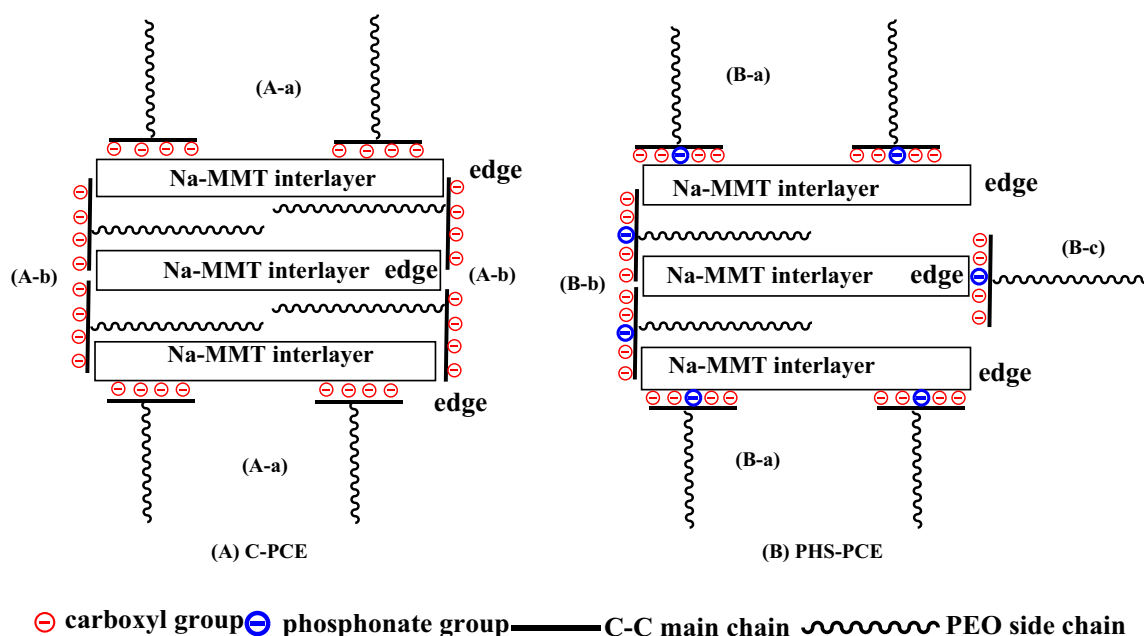

Fig. 21 Schematic diagram of interaction between PCE and MMT (**A**) C-PCE; **B** P-PCE

affected by clay. On the other hand, the presence of PHS-PCE adsorbed on the edges of clay impedes the intercalation of the superplasticizer by MMT.

(4) In engineering practice, PHS-PCE's superior dispersing ability can significantly improve the workability of concrete, which is beneficial to streamline construction processes. However, the employment of MOEP can bring high cost for PHS-PCE synthesis. Further research and optimization may help mitigate these challenges and enhance the cost-effectiveness of the method.

Declarations

References

1. Li X, Zheng D, Zheng T et al (2017) Enhancement clay tolerance of PCE by lignin-based polyoxyethylene ether in montmorillonite-contained paste. J Ind Eng Chem 49:168–175. https://doi.org/10.1016/j.jiec.2017.01.024

2. Lei L, Plank J (2014) A study on the impact of different clay minerals on the dispersing force of conventional and modified vinyl ether based polycarboxylate superplasticizers. Cem Concr Res 60:1–10. https://doi.org/10.1016/j.cemconres.2014.02.009

3. Wang Z, Wu H, Xu Y et al (2014) Inhibition mechanism of clays on applying performance of polycarboxylate superplasticizer (in Chinese). J Build Mater 17:234–238. https://doi.org/10.3969/j.issn.1007-9629.2014.02.009

4. Wang Z, Kao Y, Wang L et al (2015) Effect and Mechanism of Single Mineral Clay on Dispersibility of Polycarboxylate Superplasticizer (in Chinese). J Build Mater 18(05):879–887. https://doi.org/10.3969/j.issn.1007-9629.2015.05.029

5. Borralleras P, Segura I, Aranda M et al (2019) Influence of the polymer structure of polycarboxylate-based superplasticizers on the intercalation behavior in montmorillonite clays. Constr Build Mater 220:285–296. https://doi.org/10.1016/j.conbuildmat.2019.06.014

6. Ng S, Plank J (2012) Interaction mechanism between Na montmorillonite clay and MPEG-based polycarboxylate superplasticizers. Cem Concr Res 42:847–854. https://doi.org/10.1016/j.cemconres.2012.03.005

7. Lei L, Plank J (2014) Synthesis and properties of a vinyl ether-based polycarboxylate superplasticizer for concrete possessing clay tolerance. Ind Eng Chem Res 53:1048–1055. https://doi.org/10.1021/ie4035913

8. Xu H, Sun S, Wei J et al (2015) β-Cyclodextrin as pendant groups of a polycarboxylate superplasticizer for enhancing clay tolerance. Ind Eng Chem Res 54(37):9081–9088. https://doi.org/10.1021/acs.iecr.5b02578

9. Li Y, Guo H, Zhang Y et al (2014) Synthesis of copolymers with cyclodextrin as pendants and its end group effect as superplasticizer. Carbohydr Polym 102:278–287. https://doi.org/10.1016/j.carbpol.2013.11.044

10. Wu X, Niu X, Gao Q et al (2018) Effect of polycarboxylate superplasticizers containing AMPS on clay sensitivity (in chinese). J Build Mater 21:1519. https://doi.org/10.3969/j.issn.1007-9629.2018.01.003

11. Ma J, Wang T, Qi S et al (2018) Effects of structure on the properties of low-molecular-weight superplasticizer using phosphonate as the adsorption group. Colloid Polym Sci 296(3):503–514. https://doi.org/10.1007/s00396-018-4272-4

12. Stecher J, Plank J (2019) Novel concrete superplasticizers based on phosphate esters. Cem Concr Res 119:36–43. https://doi.org/10.1016/j.cemconres.2019.01.006

13. Wang P (2016) Study on the synthesis Process of phosphate-polycarboxylate superplasticizer (in Chinese) dissertation. Tianjin University, Tianjin

14. Checchetti A, Lanzo J (2015) Qualitative measurement of pH and mathematical methods for the determination of the equivalence point in volumetric analysis. World J Chem Educ 3(3):64–69. https://doi.org/10.12691/wjce-3-3-2

15. Plank J, Sachsenhauser B, De Reese J (2010) Experimental determination of the thermodynamic parameters affecting the adsorption behavior and dispersion effectiveness of PCE superplasticizers. Cem Concr Res 40(5):699–709. https://doi.org/10.1016/j.cemconres.2009.12.002

16. Zingg A, Winnefeld F, Holzer L et al (2009) Interaction of polycarboxylate-based superplasticizers with cements containing different C_3A amounts. Cem Concr Compos 31(3):153–162. https://doi.org/10.1016/j.cemconcomp.2009.01.005

17. Lin X, Liao B, Zhang J et al (2019) Synthesis and characterization of high-performance cross-linked polycarboxylate superplasticizers. Constr Build Mater 210:162–171. https://doi.org/10.1016/j.conbuildmat.2019.03.185

18. Liu Z, Fu H, Zhang L et al (2016) Synthesis of itaconic acid-sodium allysulfonate-sodium hypophosphite copolymer and evaluation of its scale and corrosion inhibition performance. Desalin Water Treat 57(13):5740–5752. https://doi.org/10.1080/19443994.2015.1008580

19. Abile R, Russo A, Limone C et al (2018) Impact of the charge density on the behavior of polycarboxylate ethers as cement dispersants. Constr Build Mater 180:477–490. https://doi.org/10.1016/j.conbuildmat.2018.05.276

20. He Y, Shu X, Wang X et al (2020) Effects of polycarboxylates with different adsorption groups on the rheological properties of cement paste. J Dispersion Sci Technol 41(6):873–883. https://doi.org/10.1016/j.conbuildmat.2018.05.276

21. Feng P, Zhang G, Zhang W et al (2022) Comparison of ester-based slow-release polycarboxylate superplasticizers with their polycarboxylate counterparts. Colloids Surf A 633:127878. https://doi.org/10.1016/j.colsurfa.2021.127878

22. Pourchet S, Liautaud S, Rinaldi D et al (2012) Effect of the repartition of the PEG side chains on the adsorption and dispersion behaviors of PCP in presence of sulfate. Cem Concr Res 42(2):431–439. https://doi.org/10.1016/j.cemconres.2011.11.011

23. Zhang Y, Kong X (2015) Correlations of the dispersing capability of NSF and PCE types of superplasticizer and their impacts on cement hydration with the adsorption in fresh cement pastes. Cem Concr Res 69:1–9. https://doi.org/10.1016/j.cemconres.2014.11.009

24. Liu X, Wang Z, Zhu J et al (2014) Synthesis, characterization and performance of a polycarboxylate superplasticizer with amide structure. Colloids Surf A 448:119–129. https://doi.org/10.1016/j.colsurfa.2014.02.022

25. Plank J, Hirsch C (2007) Impact of zeta potential of early cement hydration phases on superplasticizer adsorption. Cem Concr Res 37(4):537–542. https://doi.org/10.1016/j.cemconres.2007.01.007

26. Akhlaghi O, Aytas T, Tatli B et al (2017) Modified poly(carboxylate ether)-based superplasticizer for enhanced flowability of calcined clay-limestone-gypsum blended Portland cement. Cem Concr Res 101:114–122. https://doi.org/10.1016/j.cemconres.2017.08.028

27. Yang Z, Yu M, Liu Y et al (2019) Synthesis and performance of an environmentally friendly polycarboxylate superplasticizer based on modified poly(aspartic acid). Constr Build Mater 202:154–161. https://doi.org/10.1016/j.conbuildmat.2018.12.148

28. Plank J, Sachsenhauser B (2009) Experimental determination of the effective anionic charge density of polycarboxylate superplasticizers in cement pore solution. Cem Concr Res 39:1–5. https://doi.org/10.1016/j.cemconres.2008.09.001

29. Sowoidnich T, Rachowski T, Rößler C et al (2015) Calcium complexation and cluster formation as principal modes of action of polymers used as superplasticizer in cement systems. Cem Concr Res 73:42–50. https://doi.org/10.1016/j.cemconres.2015.01.016

30. Xue Q, Pang Y, Pan L et al (2018) Effect of water-reducing chemical admixtures on early hydration of cement. Adv Cem Res 20:93–100. https://doi.org/10.1680/adcr.2008.20.3.93

31. Jansen D, Neubauer J, Goetz N et al (2012) Change in reaction kinetics of a Portland cement caused by a superplasticizer-calculation of heat flow curves from XRD data. Cem Concr Res 42(2):327–332. https://doi.org/10.1680/adcr.2008.20.3.93